# 12.5kW Advanced Electric Propulsion System Thruster Development Testing

Jonathan Zubair<sup>1</sup>, Hoang Dao<sup>2</sup>, Nicholas Branch<sup>3</sup>, Derek Inaba<sup>4</sup> and Benjamin Welander.<sup>5</sup>

Aerojet Rocketdyne, Redmond, WA, USA

Jason Frieman<sup>6</sup>, Hani Kamhawi<sup>7</sup> NASA Glenn Research Center, Cleveland, OH, USA

Robert Lobbia<sup>8</sup>, Richard Hofer<sup>9</sup>

Jet Propulsion Laboratory, California Institute of Technology, Pasadena, CA, USA

Since 2012, NASA has been developing the 12.5kW Hall Effect Rocket with Magnetic Shielding (HERMeS) thruster to serve the need for deep space propulsion. Aerojet Rocketdyne (AR) is developing the HERMeS Hall Current Thruster (HCT) into a flight capable design through the Advanced Electric Propulsion System (AEPS) program. In execution of this program, Aerojet Rocketdyne has designed, built and begun test of two Engineering Test Unit (ETU) HCTs, designated ETU-1 and ETU-2. This paper presents some of the preliminary results from the ETU-1 thruster, and draws comparisons to previous HERMeS Technology Demonstration Units (TDUs) and the ETU-2 characterization unit. The ETU-1 thruster serves to evaluate the ETU design against dynamic and thermal environments while ETU-2 undergoes operational characterization and wear testing. The thruster has been exposed to acceptance and qualification-level vibration and shock testing, and has undergone acceptance and characterization hot-firing to evaluate thruster performance after exposure to dynamic environments. The results have demonstrated that the dynamic environments have not had an adverse effect on performance, and demonstrated that stability and operating characteristics remain unaffected. Together, ETU-1 and ETU-2 HCTs have demonstrated operating performance and characteristics in-family with each other and with the NASA **HERMeS Technology Demonstration Units.** 

#### **Nomenclature**

AEPS = Advanced Electric Propulsion System

AR = Aerojet Rocketdyne EP = Electric Propulsion ETU = Engineering Test Unit

<sup>&</sup>lt;sup>1</sup> Electric Thruster Engineer, Jonathan.Zubair@Rocket.com

<sup>&</sup>lt;sup>2</sup> Senior Electric Thruster Engineer

<sup>&</sup>lt;sup>3</sup> Electric Thruster Engineer

<sup>&</sup>lt;sup>4</sup> Aerojet Rocketdyne AEPS Thruster Test Lead

<sup>&</sup>lt;sup>5</sup> Aerojet Rocketdyne AEPS Thruster Lead

<sup>&</sup>lt;sup>6</sup> Research Engineer, Electric Propulsion Systems Branch, Member AIAA

<sup>&</sup>lt;sup>7</sup> NASA AEPS Test Lead, Electric Propulsion Systems Branch, Associate Fellow AIAA.

<sup>&</sup>lt;sup>8</sup> Engineer, Electric Propulsion Group, Senior Member AIAA

<sup>&</sup>lt;sup>9</sup> NASA AEPS Thruster Lead, Electric Propulsion Group, Associate Fellow AIAA.

GRC = Glenn Research Center

HERMeS = Hall Effect Rocket with Magnetic Shielding

IFPC = Inner Front Pole Cover I<sub>SP</sub> = Specific Impulse

JPL = Jet Propulsion Laboratory LIF = Laser Induced Fluorescence

 $LN_2$  = Liquid Nitrogen

OFPC = Outer Front Pole Cover

RTD = Resistive Temperature Detector

TC = Thermocouple

TDU = Technology Development Unit

TVAC = Thermal Vacuum VF-5 = Vacuum Facility-5 WCC = Worst Case Cold WCH = Worst Case Hot

#### I. Introduction

Solar Electric Propulsion (SEP) has been identified as an enabling technology by NASA's Human Exploration and Operations Mission Directorate and Science Mission Directorate for near term and future deep space missions [1]. SEP systems have significantly higher specific impulse ( $I_{SP}$ ) than traditional chemical propulsion systems, and can therefore reduce the size and mass impacts that propulsion systems have on mission architectures. High-power SEP will be used in the Artemis lunar exploration program, specifically in the design of the Lunar Gateway. The first component of the Lunar Gateway, the Power and Propulsion Element , currently under development by Maxar Technologies, will notionally implement a 40 kW SEP system, that will utilize two AEPS HCTs, as shown in Figure 1 [2]. The capability of the AEPS HCTs may also make them suitable as a potential propulsion method for providing logistics services to the deep space gateway, as well as other commercial and exploration interests [3].

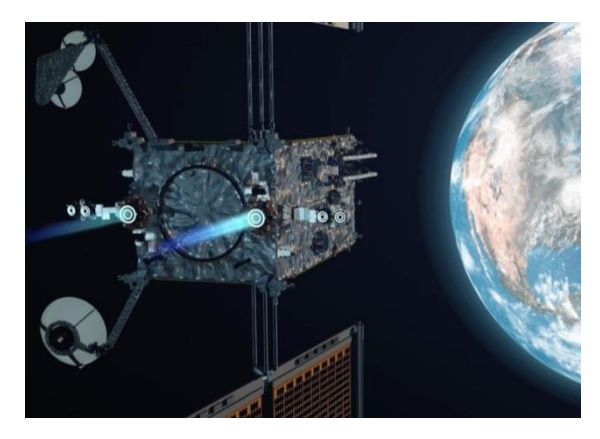


Figure 1: Maxar Power and Propulsion Element Rendering

The AEPS Engineering Test Unit (ETU) thruster design is derived from the NASA Hall Effect Rocket with Magnetic Shielding (HERMeS) Technology Development Units (TDU). Since 2012, the NASA Glenn Research Center (GRC) and the Jet Propulsion Laboratory (JPL) have been maturing the 12.5kW HERMeS thruster as a building block of this larger 40kW SEP capability. The NASA TDU thrusters have undergone extensive environmental, characterization, and wear testing as described in detail in Refs. [4] [5] [6] [7] [8] [9] [10] [11] [12] [13] [14] [15].

The HERMeS TDU design features a center-mounted cathode which is electrically tied to the thruster's graphite pole covers, as well as a magnetic field topology that shields the discharge chamber walls from erosion. Zero-erosion technology was enabled by magnetic shielding which was first demonstrated by Aerojet Rocketdyne and JPL on the BPT-4000 (XR-5) [16]. This magnetic field topology eliminates discharge chamber erosion as a primary life-limiting mechanism, with the TDU-3 Long Duration Wear Test demonstrating pole cover erosion rates low enough to satisfy the 23 khr AEPS operational life requirement [5] [7]. The Aerojet Rocketdyne ETU HCTs preserve these key design features and have iterated the design to improve the dynamic stress capability, reduce thermally induced stresses,

improve manufacturability, and meet spacecraft interface requirements [17]. An image of the HERMeS TDU and ETU HCT are provided in Figure 2 for comparison.

The ETU thruster design is capable of operating over a large range of electrical inputs. The thruster is nominally operated at a constant discharge current of 20.83A and nominally throttles between discharge voltages of 300V to 600V. Furthermore, at the 300V discharge, the corresponding discharge current can be throttled from 8.6A to 20.83A. Thruster operation and stability has also been demonstrated for centerline magnetic field strengths varying from 75% to 125% of the nominal. Furthermore, the ETU design has been demonstrated to operate at the 13.1kW contingency discharge power condition at setpoints of either 630V/20.83A or 600V/21.87A.

The ETU HCTs are intended to provide an initial assessment of a flight-like HCT design and to identify issues arising during manufacturing, assembly, and test, prior to the final design phase. Two ETU HCTs are being tested in parallel to assess design compliance to the various AEPS HCT requirements. The ETU-1 HCT is being used to evaluate the ETU design against both dynamic and thermal environments, while the ETU-2 HCT is being used to more fully characterize the thruster operating behavior and gather erosion data. The build and test of the two ETU HCTs mirrors the approach that will be taken for thruster qualification, wherein two units will be built and tested in parallel in order to compress the overall duration of the qualification program [17].

This paper will provide an overview of the testing completed by the ETU-1 HCT so far and will provide some preliminary results from the test campaign. These preliminary results are compared against the ETU-2 thruster and previous TDU data and AEPS program requirements to provide an initial assessment of the capability of the ETU design.



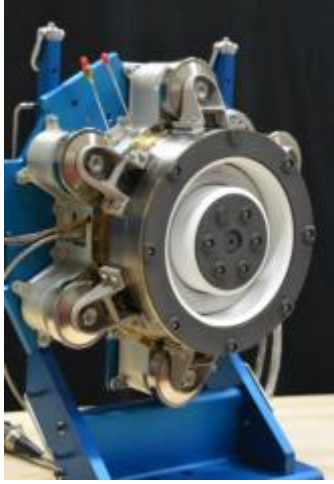


Figure 2: The NASA HERMeS TDU HCT (left) and AR AEPS ETU HCT (right).

### II. ETU-1 Testing Overview

The ETU-1 HCT environmental test sequence is provided in Figure 3. The test sequence consists of an initial vibration test to evaluate the workmanship of the thruster build and to gain insight into the dynamic response of the thruster. This was followed by an initial hot-firing characterization test to assess the performance and operating characteristics of the ETU design and to compare it to previous TDU data. This test also served to provide a baseline of ETU performance prior to qualification-level vibration and shock environments. Following this dynamic test sequence, the thruster underwent another hot-fire acceptance and characterization test to verify that the environments did not adversely affect thruster performance. At the time of this writing, the ETU-1 thruster is being prepared for thermal vacuum (TVAC) testing, which will evaluate the thruster performance at the worst case hot and cold (WCH and WCC) environments. Following this environmental test sequence the thruster shall be disassembled, inspected, and reassembled to thoroughly evaluate the effects of the various environments on the thruster piece parts and components. In addition to the tests provided in Figure 3 and the description above, various functional tests were performed throughout the campaign. These included dimensional inspections to evaluate gross changes in component positions, as well as electrical functionals and magnetic field mapping to verify continuity of thruster component operation. Detailed descriptions of the ETU-1 thruster and test setups are provided in the sections below.

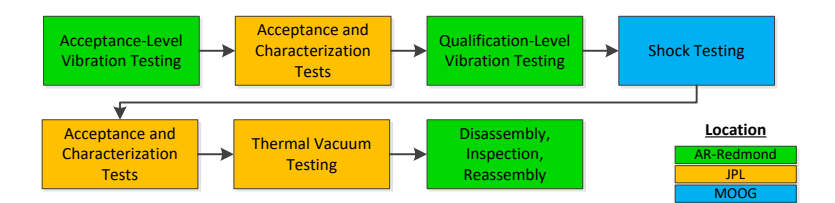


Figure 3: ETU-1 Environmental and Hot-Fire Testing Logic

# A. ETU-1 HCT Instrumentation and Configuration

The ETU-1 HCT is instrumented with 15 type-K thermocouples (TCs), which are mounted throughout the thruster volume; including TCs embedded in the inner and outer coil assemblies. In addition to TCs, the ETU HCT design uses four resistive temperature detectors (RTDs) to provide thermal telemetry of the thruster backpole and inner and outer plasma screens. For hot-fire testing, the ETU HCTs use a development level hollow cathode assembly which provides the same plasma wetted geometry as the notional qualification and flight cathode assemblies and retains key features such as the graphite keeper and BaO emitter; however, these cathodes are not designed for the dynamic environments experienced by ETU-1 and, therefore, the cathode assembly was removed for these portions of the test campaign. Flight-like cathodes will be tested against the dynamic requirements of the AEPS program during later cathode stand-alone environmental testing as well as during subsequent thruster qualification efforts.

#### B. Vibration Testing Setup and Methodology

Vibration tests were performed at Aerojet Rocketdyne's Redmond, WA facility, to a set of two levels: acceptance and qualification. For both tests, the ETU-1 HCT was instrumented with 11 response accelerometers. Additionally, two control accelerometers were mounted to the vibration fixture to provide control input to the shaker table. Vibration testing was conducted along the three orthogonal axes identified in Figure 4. For each axis low-level sine sweep was performed before and after the random vibration test itself. Low level sine sweeps were performed in order to evaluate changes in the thruster's natural frequencies as a result of the random vibration environment. These sine sweeps were performed to the levels identified in Table 1. Random vibration testing was conducted to the amplitudes and durations specified in Table 2.

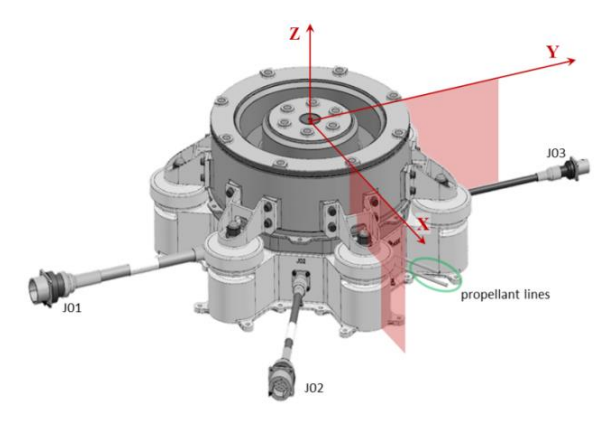


Figure 4: ETU Vibration and shock Axes

**Table 1: Low-level sine sweep parameters** 

Frequency, Hz	Intensity, g	Sweep Rate, Octave/min	
10-2000	0.5	4	

Table 2: Random vibration acceptance and qualification level test inputs

Frequency, Hz	Acceptance Level*	Qualification Level**

20	0.026 G <sup>2</sup> /Hz	$0.052~{ m G}^2/{ m Hz}$
20-50	+ 3dB/Octave	+ 3dB/Octave
50-600	$0.065  \mathrm{G}^2/\mathrm{Hz}$	$0.130  G^2/Hz$
600-2000	- 6dB/Octave	- 6dB/Octave
2000	$0.006  \mathrm{G}^2/\mathrm{Hz}$	$0.012  \mathrm{G}^2/\mathrm{Hz}$
Overall	$8.1~G_{RMS}$	$11.4~G_{RMS}$

<sup>\*</sup>Acceptance duration: 1 minute per axis, in 3 orthogonal axes

#### C. Shock Testing Setup and Methodology

Following vibration testing, the ETU-1 thruster underwent shock testing at Moog CSA's Mountain View, CA facility. The thruster was instrumented with response accelerometers at the same locations and used the same three (3) orthogonal axes as used during vibration testing. A pneumatic canon was used to administer three shock events per axis to the shock fixture. The shock response spectrum (SRS) input levels are provided in Table 3 for reference.

**Table 3: Shock response spectrum levels** 

Frequency, Hz	SRS Level (g)		
100	30		
1600	630		
10000	630		

## D. Hot-firing Characterization Tests

Hot-firing characterization testing of the ETU-1 HCT was performed at JPL in Pasadena, CA. All hot-fire testing was performed in the Owens vacuum chamber to the nominal sequence provided in Figure 5. Following the initial magnet, cathode, and thruster outgassing sequences, a series of reference firings were performed at the discharge power conditions outlined in Table 4. At each reference firing setpoint, a faraday probe sweep was performed at several axial distances from the thruster exit plane. The thruster thermal performance was then evaluated with thermal equilibrium runs at the 12.5 kW power setting at both the nominal and 125% magnetic field settings. Lastly the stability of the thruster was evaluated with a discharge current, discharge voltage and magnetic field (IVB) sweep. This IVB sweep was performed over a discharge voltage range of 150V to 630V at the discrete magnetic field settings of 75%, 87.5%, 100%, 112.5%, and 125% of the nominal in order to create an IVB map. Details regarding the setup of the Owen's facility and the test equipment used are provided in the sections below.

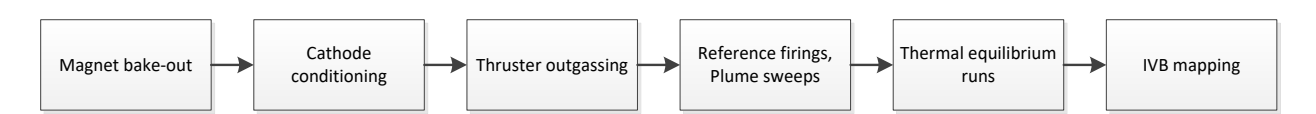


Figure 5: ETU-1 hot-firing characterization test flow

Table 4: AEPS ETU reference firing operating conditions

ID	Discharge Voltage, V	Discharge Current, A	Discharge Power, W
REF-300	300	20.83	6250
REF-400	400	20.83	8333
REF-500	500	20.83	10417
REF-600	600	20.83	12500

#### 1. Owens Vacuum Facility

The Owens vacuum chamber is a 3m diameter by 8.6m long cylindrical vacuum chamber that is cryogenically pumped with three 48" CVI cryo-pumps and nine custom LN<sub>2</sub> shrouded cryo-sails. The chamber walls downstream

<sup>\*\*</sup> Qualification duration: 2 minutes per axis, in 3 orthogonal axes

of the thruster are lined with graphite plates to minimize ion sputtering of chamber surfaces. An additional graphite structure at the downstream end of the chamber protects the chamber walls from erosion and is cooled using  $LN_2$  to remove power deposited into the graphite by the ion beam [12]. Facility pressure was measured using two Stabil-Ion gauges, calibrated for measurement on xenon. Stabil Ion Gauge 1 was located 1 meter radially from the thruster and was axially located in thruster exit plane. The second gauge was mounted directly below the thruster in the exit plane, and oriented axially downstream. The chamber demonstrated a zero flow base pressure of  $<5*10^{-7}$  Torr Xe and at no point during testing did the chamber exhibit pressures greater than  $5*10^{-5}$  Torr-Xe. This facility has previously been used to test a wide range of EP devices including the HERMeS TDU-2 thruster whose testing in the Owens chamber is described in Refs. [12] [14].

Cathode heater, keeper, magnet, and discharge power were supplied to the thruster with computer controlled commercial laboratory power supplies. The ETU-1 thruster utilized the same Xenon Feed System that was previously used for TDU testing, wherein high purity xenon was provided to the anode and cathode using computer controlled mass flow controllers.

#### 2. Thrust Stand

The JPL Owens Vacuum Chamber employs a water cooled inverted pendulum thrust stand to measure thrust. The thrust stand was calibrated before and after each reference firing of the ETU-1 thruster by cycling a series of calibrated weights and recording the resultant change in the output signal from the LVDT on the Opto-22 data acquisition system.

# 3. Faraday Probe System

During testing, the Owens facility was equipped with a faraday Probe mounted on coupled radial and axial motion stages. When not in use, the probe was parked outside the thruster plume near the wall of the chamber. During operation, the probe is swept via computer control across the plume radially, maintaining a constant distance downstream of the thruster exit plane.

#### 4. Data Acquisition

A JPL Opto-22 data acquisition system was used to record the majority of test telemetry. Low-speed telemetry included the calibrated sense lines for the DC power supplies, including current and voltage telemetry for the inner and outer magnets, cathode heater, keeper, and thruster discharge. Additional low-speed telemetry included cathode to ground voltage, anode and cathode mass flow rates, facility pressure, and TC data.

Additionally, two digital oscilloscopes along with appropriate current and voltage probes were used throughout testing to capture high-speed ignition and steady state telemetry of the thruster. A Teledyne LeCroy HDO8038 12-bit oscilloscope was used to monitor steady state, peak-to-peak waveforms of the anode, cathode, body, and keeper currents, as well as anode to cathode, cathode to ground, and keeper to cathode potentials. A Tektronix oscilloscope was used during cathode startup to capture the keeper to cathode and cathode to ground potentials and the keeper and anode currents, and was triggered on the rising keeper current. During HCT ignition, the Tektronix was also used to capture keeper to cathode and anode to cathode potentials and keeper and anode currents, and was triggered on the raising of anode current to 10A.

# **III. ETU-2 Testing Overview**

The ETU-2 test sequence conducted to date consisted of an initial reference firing and characterization test followed by two short duration wear test blocks. The characterization test evaluated the performance, stability and thermal characteristics of the thruster, as well as facility effects on the overall performance of the thruster. The characterization tests were followed by a two block wear test. To date, all ETU-2 thruster testing has been conducted in the VF-5 vacuum test facility at the NASA Glenn Research Center (GRC). At the time of this writing, the ETU-2 testing campaign is currently being prepared for Laser Induced Fluorescence (LIF) characterization, and subsequently, extended wear testing.

Frieman et al. provide a detailed overview of the test setup and sequence, facility equipment and diagnostics, and characterization and wear test results [4] [18]. A brief summary of the ETU-2 thruster configuration and test sequence is provided here.

#### A. ETU-2 HCT Instrumentation

The AEPS ETU-2 HCT is instrumented with 30 type-K thermocouples (TC), which are mounted throughout the thruster volume; including TCs embedded in the inner and outer coil assemblies as well as the inner and outer discharge chamber walls. The ETU-2 HCT also uses four RTDs to collect thermal telemetry of the thruster backpole

and inner and outer plasma screens. During the initial reference firing and characterization test, radiator fins were installed on the thruster as shown in Figure 6Error! Reference source not found., but were removed at the start of the wear test.

Since the magnetic field topology mitigates erosion of the discharge chamber walls, TDU testing has identified that erosion of the inner and outer front pole covers (IFPC and OFPC) as the next life-limiting mechanism for the HERMeS design. In order to assess pole cover erosion during the wear test segments, polished pole covers similar to those used in the HERMeS TDU-3 long duration wear test (LDWT) were installed on the ETU-2 thruster [LDWT]. These pole covers were polished in order to minimize surface roughness, and to provide a smooth baseline measurement for pre-test profilometry. Additionally, two graphite masks were installed on the IFPC and four were installed on the OFPC to preserve reference surfaces for post-test profilometry. New pole covers were installed for each segment of the wear test block. The configuration of the ETU-2 HCT for both reference firing and wear testing can be seen in Figure 6Error! Reference source not found.



Figure 6: ETU-2 HCT with (left) radiator fins installed prior to reference firing and (right) wear pole covers installed for wear testing.

#### B. Reference Firing and Characterization Test Description

ETU-2 reference firing sequence included all set-points included in the ETU-1 testing campaign, but also included the 630V/20.83A and 600V/21.87A setpoints for an evaluation of thruster performance during contingency operations. Additionally, the nominal reference setpoints were re-performed with the magnetic field polarity reversed. Once reference firing was completed, the thruster entered the extended characterization test sequence. The results of these characterizations tests are presented in detail in Ref. [4].

#### C. Short Duration Wear Test Description

The short duration wear test was broken into two blocks, which evaluated thruster wear at different operating conditions. The first wear block was conducted at the primary flight condition of 600V/20.83A, at the nominal magnetic field setting; 253.9 hours were accumulated at this setpoint. The second wear block was conducted at the 300V/20.83A setpoint at 125% of the nominal magnetic field setting. This setpoint was found to produce the highest measured erosion rates during TDU testing, and was selected to establish an upper bound on erosion rates for the ETU design [7]. 471.7 hours were accumulated at this condition. Prior to and following each wear block a reference firing and plume mapping was performed at the nominal reference firing setpoints to quantify any changes to thruster performance as a result of the wear blocks.

#### IV. ETU-1 Testing Results and Discussion

## A. Vibration and Shock Testing Results

The initial vibration test served as a workmanship check of the ETU-1 thruster build. An image of the ETU-1 HCT installed on the vibration table shaker head is provided in Figure 7. No test article issues were identified, but this test did serve to demonstrate that the original vibration fixture was inadequate for qualification-level testing and prompted

a new fixture to be designed and built. Following acceptance testing, the thruster underwent a visual inspection, electrical functionals, and magnet mapping. No appreciable defects were observed in any of the thruster components or in the electrical functionals. Measurements of the magnetic field topology demonstrated no change across dynamic testing.

In general the qualification-level vibration test exhibited similar response traits to those exhibited in the acceptance-level test. Thruster resonances and anti-resonances were observed near the same frequencies between the two levels. Only very slight shifts in the first natural frequencies of the thruster were observed during the pre and post random vibration low-level sine sweeps. These shifts were attributed to working-in of the isolators at the previously untested loads. Following vibration testing it was determined that the shock isolators used for ETU testing were stiffer than anticipated. The result was that the isolators transmitted higher loads to the thruster assembly downstream of the isolators. The data from these tests was used to refine the ETU structural model.

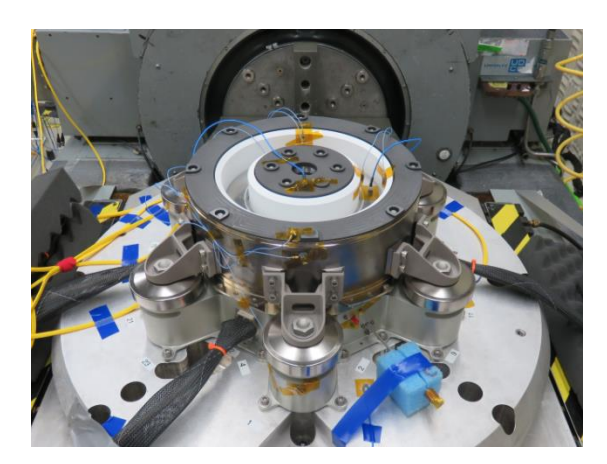


Figure 7: ETU-1 HCT during initial vibration testing.

#### E. Hot-firing Characterization Testing Results

The initial reference firing and characterization test of the ETU-1 thruster was performed in August of 2019. This test represented the first ignition of the ETU HCT as part of the AEPS program. An image of the ETU-1 HCT firing in the Owens chamber is provided in Figure 1. The thruster returned to JPL for its second round of acceptance and characterization testing following qualification-level dynamic environments testing in February of 2020.

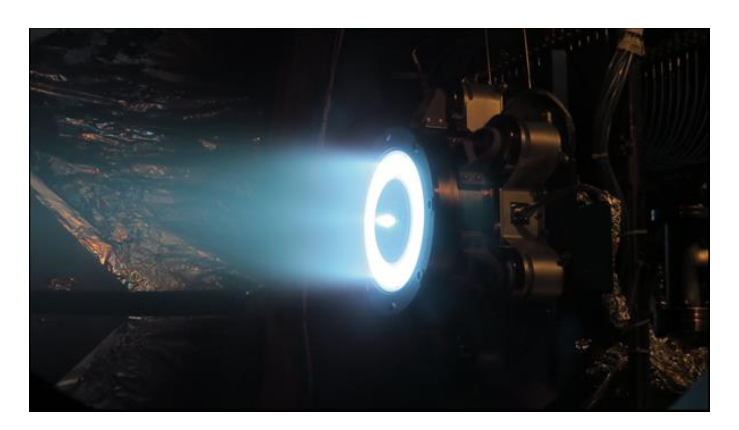


Figure 8: ETU-1 HCT firing at the JPL Owen's Vacuum Chamber

# 1. Reference Firing

The reference firing results for both pre and post-dynamic environments testing are presented in Table 1, along with TDU data collected in the Owens chamber. The reported thrust data has been corrected for thrust stand thermal drift as well as desired power offsets. The performance metric uncertainties are expected to be similar to those described for previous TDU testing in the Owens Chamber [12]. As is evident from the results, the ETU-1 thruster shows similar performance to the TDU-2 thruster both prior to and following exposure to dynamic environments. Although the thrust and specific impulse of the post-dynamic environments reference firings are lower across all

reference firing setpoints, the results are within the expected uncertainty of the measurement. In addition, the ion current profiles taken during the faraday probe sweeps at the different reference firing setpoints demonstrates very little change as a result of exposure to the dynamic environments, as shown in Figure 9.

Table 5: ETU-1 reference firing thrust and specific impulse results

			Thrust [mN]			
ID	Discharge Voltage, V	Discharge Current, A	TDU-2 (JPL)	ETU-1 (Pre-Environ.)	ETU-1 (Post-Environ.)	ETU-2 (GRC VF-5)
REF-300	300	20.83	398	398	390	396
REF-400	400	20.83	478	477	474	479
REF-500	500	20.83	544	548	544	545
REF-600	600	20.83	608	613	608	610
			Total Specific Impulse [s]			
REF-300	300	20.83	2021	2019	1981	1957
REF-400	400	20.83	2366	2364	2355	2315
REF-500	500	20.83	2568	2635	2623	2572
REF-600	600	20.83	2883	2896	2882	2807

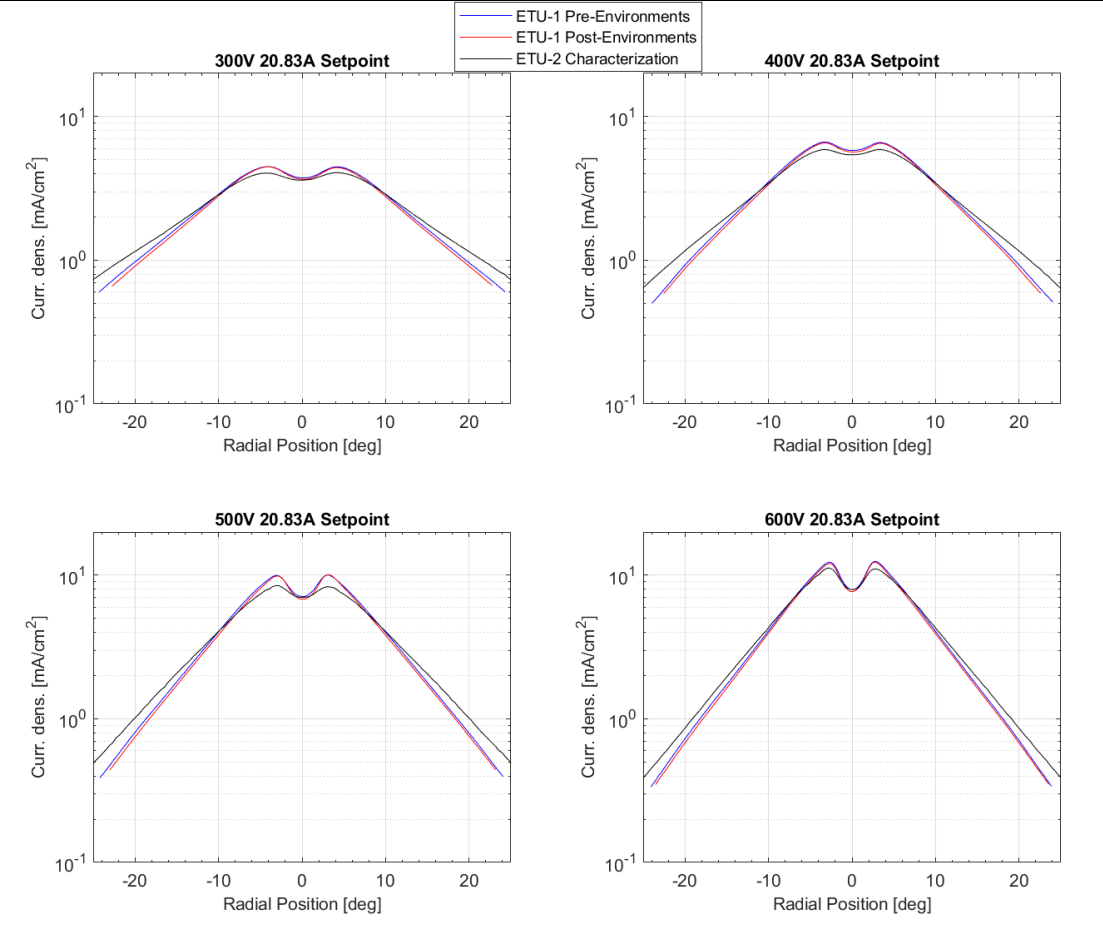


Figure 9: ETU-1 faraday probe sweeps prior to and following qualification-level dynamics testing.

Figure 9 shows the ion current density profiles for the ETU-1 thruster acquired pre and post environmental testing, as well for the ETU-2 thruster as acquired during characterization testing magnetic mapping operations. The ETU-1 results show good agreement with the ETU-2 profile, but do demonstrate increased peak ion densities near the thrust vector axis, and reduced ion current densities in the tails. Notably, the Faraday probe in the GRC VF-5 facility was located 33% further downstream than the Owens Faraday probe; this is corrected for in the visualized data using a distance squared law. To sweep the Faraday probe, the Owens test facility employs a linear motion stage in contrast to the VF-5 radial motion stage. No effort is made here to correct for possible differences introduced by the variation in Faraday probe setup, Faraday probe geometry and design, nor test facility effects such as pressure.

## 2. IVB Mapping

In addition to the performance and plume data, IVB sweeps were performed at the nominal flow rate required to maintain the 600V/20.83A reference setpoint. The IVB maps for testing prior to and following qualification-level dynamics testing is provided in Figure 10. The 3-D surfaces map the discharge current, voltage, and magnetic field, while the surface color represents the normalized root mean square of the discharge current oscillations. In general the pre and post dynamic responses are quite similar with only a slight increase in the discharge current oscillations evident near the 300V, 112.5% to 125% magnetic field setpoint.

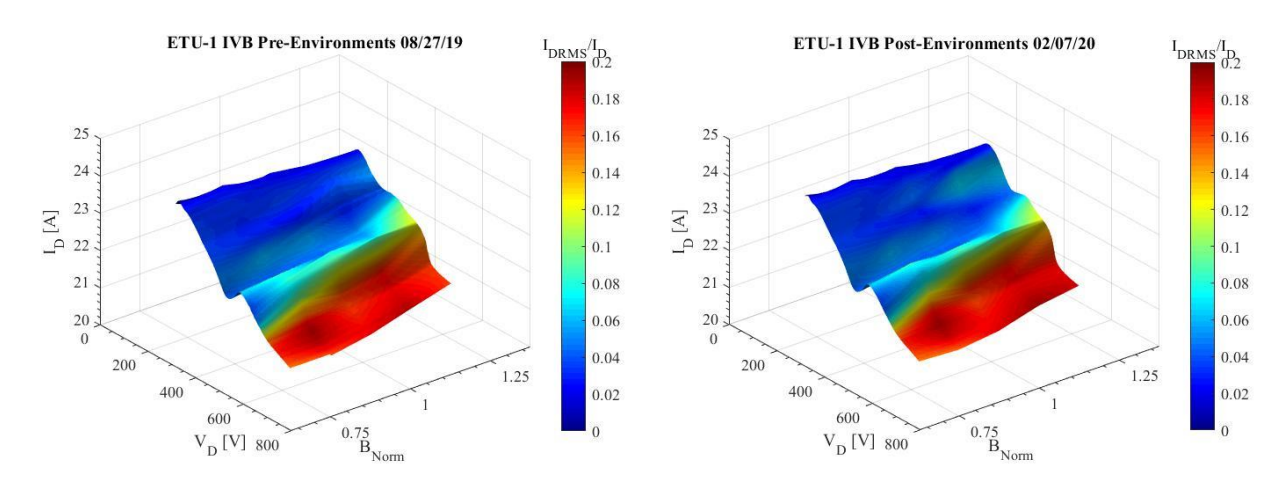


Figure 10: ETU-1 IVB maps (a) prior to and (b) following qualification-level dynamics testing

# V. Conclusions

The ETU-1 and ETU-2 test campaigns have so far demonstrated key operating performance and characteristics of the ETU design. ETU-1 environmental testing has successfully exposed the ETU thruster to acceptance and qualification level random vibration testing and shock environments on the thruster body assembly. Acceptance and characterization firing prior to and following dynamic testing has demonstrated very little effect in operating performance or stability across the nominal discharge power range. Furthermore, the data demonstrates that this thruster performance is in family with TDU-2 testing in the Owens chamber. The ETU-1 test campaign has expanded the understanding of the ETU design's operational characteristics. Thruster performance was evaluated at the nominal and contingency discharge powers as well as at magnetic field settings varying from 75% to 125% of the nominal. These results coupled with IVB mapping demonstrate the thruster's stability over a broad range of center-line magnetic field strengths.

Once testing activities resume, the ETU thrusters will finish the rest of their campaigns. For ETU-1, this will constitute thermal vacuum cycle (TVAC) testing using the same thermal shroud and test setup as described for TDU-2 [12]. The TVAC testing will expose the thruster to 12 thermal cycles to the expected WCC and WCH qualification temperatures. As mentioned previously, standalone environmental testing of a cathode prior to the qualification thruster build, shall demonstrate in a similar manner the cathode's ability to survive dynamic, thermal, and mission ignition requirements. The successful completions of these tests will demonstrate that the AEPS design is likely to survive the dynamic rigor of launch and the thermal extremes of deep space operation. The ETU-2 thruster will undergo additional characterization in the form of LIF testing. This data shall be used to refine and validate the

modeling work that NASA has been undertaking and will allow for another comparison of ETU characteristics to those of the TDU thrusters [8].

In addition to the future testing described above, the dynamic and thermal data collected during the ETU testing campaigns is currently being used to anchor and mature the ETU analytical models. These models will be used to refine the final design of the HCT as the program moves towards its critical design review.

## Acknowledgements

The execution of the AEPS HCT program has been made possible through the contributions of countless team members across Aerojet Rocketdyne, NASA GRC, and JPL. The authors would like to thank all of the individuals across these organizations who have supported the build, analysis, and test of the ETU HCTs, and who are working towards the successful qualification and flight of AEPS thrusters.

#### References

- [1] B. K. Smith, M. L. Nazario and C. C. Cunningham, Solar Electric Propulsion Vehicle Demonstration to Support Future Space Exploration Missions, Cleveland, OH, 2012.
- [2] [Online]. Available: investor.maxar.com/investor-news/press-release-details/2019/Maxar-Selected-to-Build-Fly-First-Element-of- NASAs-Lunar-Gateway/default.aspx.
- [3] J. F. Horton, C. B. Reynolds, N. Rodney, S. F. William, T. Kokan and D. Morris, "Gateway Logistics Services Using High TRL Advanced Propulsion and Flight Proven ISS Cargo Elements," 2020.
- [4] J. D. Frieman, H. Kamhawi, W. Huang, J. Mackey, D. Ahern and P. Peterson, "Characterization Test of the 12.5-kW Advanced Electric Propulsion System Engineering Test Unit Hall Thruster," in 56th AIAA/SAE/ASEE Joint Propulsion Conference, Cleveland, Ohio, 2020.
- [5] J. D. Frieman, H. Kamhawi, J. A. Mackey, T. W. Haag, P. Y. Peterson, D. A. Herman, J. H. Gilland and R. R. Hofer, "Completion of the Long Duration Wear Test of the NASA HERMeS Hall Thruster," in *AIAA Propulsion and Energy 2019 Forum*, Indianapolis, IN, 2019.
- [6] J. D. Frieman, H. Kamhawi, P. Y. Peterson, D. Herman, J. Gilland and R. Hofer, "Impact of Facility Pressure on the Wear of the NASA HERMeS Hall Thruster," in *36th Internation Electric Propulsion Conference*, Vienna, Austria, 2019.
- [7] J. D. Frieman, H. Kamhawi, G. J. Williams, W. Huang, D. A. Herman, P. Y. Peterson, J. H. Gilland and R. R. Hofer, "Long Duration Wear Test of the NASA HERMeS Hall Thruster," in *2018 Joint Propulsion Conference*, Cincinnati, Ohio, 2018.
- [8] W. Huang, H. Kamhawi and D. A. Herman, "Ion Velocity in the Discharge Channel and Near-Field of the HERMeS Hall Thruster," in *Joint Propulsion Conference*, Cincinnati, Ohio, 2018.
- [9] W. Huang, H. Kamhawi, T. W. Haag, A. L. Ortega and I. G. Mikellides, "Facility Effect Characterization Test of NASA's HERMeS Hall Thruster," in *52nd AIAA/SAE/ASEE Joint Propulsion Conference*, Salt Lake City, Utah, 2016.
- [10] W. Huang, G. J. Williams, P. Y. Peterson, H. Kamhawi, J. H. Gilland and D. A. Herman, "Plasma Plume Characterization of the HERMeS During a 1722-hr Wear Test Campaign," in *35th International Electric Propulsion Conference*, Atlanta, Georgia, 2017.
- [11] H. Kamhawi, J. Mackey, J. Frieman, W. Huang, T. Gray, T. Haag and I. Mikellides, "HERMeS Thruster Magnet Field Topology Optimization Study: Performance, Stability, and Wear Results," in *36th International Electric Propulsion Conference*, Vienna, Austria, 2019.
- [12] R. B. Lobbia, R. W. Conversano, S. Reilly, R. R. Hofer and R. Sorensen, "Environmental Testing of the HERMeS TDU-2 Hall Thruster," in 2018 Joint Propulsion Conference, Cincinnati, Ohio, 2018.
- [13] P. Y. Peterson, H. Kamhawi, W. Huang, J. Yim, D. Herman, G. Williams, J. Gilland and R. Hofer, "NASA HERMeS Hall Thruster Electrical Configuration Characterization," in *52nd AIAA/SAE/ASEE Joint Propulsion Conference*, Salt Lake City, Utah, 2016.

- [14] J. E. Polk, R. Lobbia, A. Barriault, P. Guerrero, I. Mikellides and A. L. Ortega, "Inner Front Pole Cover Erosion in the 12.5 kW HERMeS Hall Thruster Over a Range of Operating Conditions," in *35th International Electric Propulsion Conference*, Atlanta, Georgia, 2017.
- [15] G. J. William, H. Kamhawi, M. Choi, T. W. Haag, W. Huang, D. A. Herman, J. H. Gilland and P. Y. Peterson, "WEar Trends of ther HERMeS Thruster as a Function of Throttle Point," in *35th International Electric Propulsion Conference*, Atlanta, Georgia, 2019.
- [16] I. G. Mikellides, I. Katz, R. R. Hofer, D. M. Goebel, K. d. Grys and A. Mathers, "Magnetic Shielding of the Acceleration Channel Walls in a Long-Life Hall Thruster," *Physics of Plasmas*, vol. 18, no. 3, 2011.
- [17] J. Jackson, S. Miller, J. Cassady, E. Soendker, B. Welander and M. Barber, "13kW Advanced Electric Propulsion Flight System Development and Qualification," in *36th International Electric Propulsion Conference*, Vienna, Austria, 2019.
- [18] J. D. Frieman, H. Kamhawi, W. Huang, J. Mackey, D. M. Ahern, P. Y. Peterson, J. Gilland, S. J. Hall, R. R. Hofer, D. Inaba, H. Dao, J. Zubair, J. Neuhoff and N. Branch, "Wear Test of the 12.5-kW Advanced Electric Propulsion System Engineering Test Unit Hall Thruster," in 2020 Propulsion and Energy Forum, 2020.
- [19] R. R. Hofer, J. E. Polk, M. J. Sekerak, I. G. Mikellides, H. Kamhawi, T. R. Sarver-Verhey and D. A. Herman, "The 12.5k kW Hall Effect Rocket with Magnetic Shielding (HERMeS) for the Asteroid Redirect Robotic Mission," 52nd AIAA/SAE/ASEE Joint Propulsion Conference, Vols. AIAA Paper 2016-4846, 2016.
- [21] D. A. Herman, T. A. Tofil, W. Santiago, H. Kamhawi, J. E. Polk, J. S. Synder, R. R. Hofer, F. Q. Picha, J. Jackson and M. Allen, "Overview of the Development and Mission Application of the Advanced Electric Propulsion System," in 35th International Electric Propulsion Conference, Atlanta, GA, 2017.
- [22] P. Y. Peterson, D. A. Herman, H. Kamhawi, J. D. Frieman, W. Huang, T. Verhey, D. Dinca, K. Boomer, L. Pinero, K. Criswell, S. J. Hall, A. Birchenough, J. H. Gilland, R. Hofer, J. E. Polk, V. Chaplin, R. Lobbia, C. E. Garner and M. K. Kowalkowski, "Overview of NASA's Solar Electric Propulsion Project," in *36th Internation Electric Propulsion Conference*, Vienna, Austria, 2019.
- [23] S. Stanley, M. Allen, K. Goodfellow, G. Chew, R. Rapetti, T. Tofil, D. Herman, J. Jackson and R. Myers, "Development of a 13 kW Hall thruster Propulsion System Performance Model for AEPS," in *53rd AIAA Joint Propulsion Conference*, Atlanta, Georgia, 2017.
- [24] G. F. Benavides, J. A. Mackey, D. M. Ahern and R. E. Thomas, "Diagnostic for Verifying the Thrust Vector Requirement of the AEPS Hall-Effect Thruster and Comparison to the NEXT-C Thrust Vector Diagnostic," in *2019 Joint Propulsion Conference*, Cincinnati, Ohio, 2018.
- [25] J. E. Polk and J. R. Brophy, "Life Qualification of Hall Thrusters By Analysis and Test," in *Space Propulsion* 2018 Conference, Seville, Spain, 2018.